Chapter

Analysis of the Creep and the Influence on the Modulus Improvement Factor (MIF) in Polyolefin Geocells Using the Stepped Isothermal Method

Juan Carlos Ruge, Julian Gonzalo Gomez and Carlos Andres Moreno

Abstract

The article shows the analysis of the behavior at long-term deformation of geocells for a set time period, due to its importance on the modulus improvement factor (MIF), which is considered in the design stage of a reinforced pavement structure with geocells. When inquiring into the research about the structural behavior that exists in the geocells, as well as the distribution of stresses that this generates, in order to determine how important the existence of a deformation in the geocell is. We proceeded with the sampling and execution of the test "modified stepped isothermal method (SIM) for geocells." The test was carried out under the comparison of the materials and thicknesses of the sample, with the purpose to analyze the influence on the behavior of a pavement structure. The stresses generated at the level of the granular subbase layer of a pavement are taken into account as load effects.

Keywords: creep, geocells, modulus improvement factor, stepped isothermal method

1. Introduction

One of the most common problems in road geotechnics projects is encountering subgrade soils of low carrying capacity. Multiple solutions are proposed to improve the unfavorable conditions of this type of soil; however, a large part of them can be harmful to the environment. In this sense, alternatives based on design with geosynthetics are important and allow for adequate reinforcement of the unsuitable soft subgrade as a supporting layer of the pavement structure.

However, with the implementation of geosynthetics, problems associated with the stresses experienced by the material were observed, such as UV degradation and long-term plastic deformation. These effects occur in almost all geosynthetics, even in geocells, which will be analyzed in detail in this article.

The first need to reinforce highly compressible soils arose during wartime at the beginning of the twentieth century, when the transport of heavy machinery was required. For this reason, the US Army Corps of Engineers was the first to use and

develop the cellular confinement system in the late 1970s, as a means to help build roads, runways, platforms, and others; all these solutions were made on very soft soils and under humid conditions.

The main large-scale use of this system of cellular confinement was during the Gulf War, in "Operation Desert Storm", where it transported heavy military material with speed and efficiency. For the purpose of mobilizing large troops, according to the company Geoceldas SA, the defense department of the United States "acquired 6.4 million square feet (600,000 square meters) of cellular geosynthetics for use in various military applications [1]."

In terms of its implementation in design tasks, pavement structure with geocells uses a coefficient of increase for the modules of the materials (MIF), which depends on several factors. Among these is resistance to long-term deformation of the material that makes up the panel of geocells. This generates a mechanism of confinement, which creates an apparent cohesion of the material incorporated therein. If the geocells yield, it is susceptible to losing its properties and begins to deform causing a settlement in the pavement structure, in addition to providing a deconfinement in the geocell filling material [2, 3].

Therefore, some consequences of deformation in the geocell are the reduction of the apparent cohesion in the filling material due to the loss of confinement, according to which there is a high decrease in the MIF coefficient taken into account during the design of the structure.

For these reasons, it is important to know the properties of the materials that are involved in the pavement structures and the veracity of the calculations that are made in the analyses. Therefore, when calculating the MIF, it is important to know the long-term deformation of material to give support and certainty in the analyses. Consequently, a modified test based on the SIM for geocells was developed. A test program was carried out using different samples of geocells, exposing results for each one of them.

The definition of the MIF factor refers to the material modulus with reinforcement vs. the material without reinforcement. This value is obtained at the moment of designing a structure with geocell, applying five characteristics of the material-geocell set, among which is the long-term deformation of geosynthetic. The MIF value depends on the analysis of the creep in the geocells, because if the material becomes deconfined, the increase of the modulus considered in the design will be reduced. For this reason, a safety factor is applied to the MIF, due to the creep in the geocells.

The samples were analyzed under load effects, which contemplate those generated at the level of the granular subbase layer of pavement, thus showing the feasibility of use in this layer and the possible behavior of these over its usable life.

2. Methodology

This research was based on the stepped isothermal method (SIM) which is standardized by ASTM D6992 [4, 5]. It was modified to prove the long-term deformation of the geocells and to learn the incidence that this property has when calculating the MIF, which is described as the relationship that exists between the module of a granular material confined with geocells and the same granular material without confinement, determined from Eq. (1) [6]. Basically, the adjustment on the test was based in terms of the width and length of the specimens, which depends on the type of geocell that is being analyzed.

$$MIF = \frac{E_{reinforced}}{E_{no-reinforced}} \quad (1)$$

The SIM test determines the long-term deformation of polymers by time-temperature superposition, whose effect was modified for use in polyolefin geocells. This method, known as the "time-temperature superposition principle (PSTT)," establishes that material having a viscoelastic property (V) measured in a time interval coincides with the same measurement in greater times at a lower temperature. Because this method is clearly empirical, it is defined as a principle, because not even theoretical concepts have been developed to sustain it [7].

With the aforementioned considerations, an increase in temperature according to Billmeyer [8], accelerates molecular and segmental movement, leading the system to equilibrium more quickly or "apparent equilibrium," accelerating all viscoelastic processes.

To that extent, the modification proposal is based on systematically dividing the trial into five steps, in which the temperature will be increased with a specific duration for each step. In addition to applying a constant load throughout the trial of 4.4 kN/m, the temperatures reached for each step are 21 ± 1, 44, 51, and 65°C, respectively.

The first part of the test refers to the simulation of the load exerted on the geocell at the time of compaction of the filling material. It is possible to find a mean of time-temperature superposition according to [9], a temperature of 51°C and 1 hour of testing, equivalent to 100,000 hours of use (4166 days or 11 years).

The load of 4.4 kN/m, to which the material is subjected throughout the test, replicates the force supported by the geocell in the granular subbase of a pavement structure. This necessitates implementation of a series of charges which will be imposed through weights that will transmit this force to the geocells.

Properties of the material	**Testing method**	**Unit**	**Values MARV**
Polymer density	ASTM D-1505	g/cm^3	0.935–0.965
Black smoke content	ASTM D-1603	% weight	1.5% min
Nominal thickness of the cell wall before texturing	ASTM D-5199	mm	1.1 ± 10%
Nominal thickness of the cell wall after texturing	ASTM D-5199	mm	1.52 ± 10%
Physical properties	**Testing method**	**Unit**	**Typical values**
Nominal size of the expanded cell	Measured	mm	320 × 287
Nominal area of the expanded cell	Measured	cm^2	460
Nominal size of the expanded panel	Measured	m	2,56 × 8,35
Nominal size of the expanded panel	Measured	m^2	21,04
Height of the cell	Measured	mm (in)	75(3) 100(4) 150(6) 200(8)
Resistance of the joints by ultrasound	USAGE GL-86-19	N	1065 1420 2130 2840
Ultimate resistance to joints tension	ISO 13426-1 method B	kN/m	15
Ultimate resistance to tension wide strip method	ISO 10319	kN/m	25
% of perforations per unit area	Measured	%	12±2

Table 1.
Properties of geocell type 1, Provider 1.

Physical properties	Norm	Unit	Typical values
Density of the material	ASTM D-1505	g/cm^3	0.950 ± 0.015
Thickness of the sheet (textured)	ASTM D-5199	mm	min. 1.52 ± 0.15
Black carbon content	ASTM D-1603	%	2.0 ± 0.5
Resistance to environmental cracking (ESCR)	ASTM D-1693	hours	>3000
Resistance of the joints to the takeoff	ASTM D-4437	N/cm	>150
Height of the unit		mm	150
Minimum values of resistance	ISO 13426-1 method A: shear test	kN/ joint	2.7
		kN/m	8.1
	ISO 13426-1 method B: takeoff test	kN/ joint	2.25
		kN/m	6.75
Number of cells		#/m	21.7
Diagonal length		cm	30.4
Cell area		cm^2	461
Distance between joints		mm	445
Width of the expanded unit		m	2.43
Expanded unit length		m	5.5
Coverage		m^2	13.3
Weight of the unit		kg	20.8

Table 2.
Properties of geocell type 2, Provider 2

Dimensions of the cells and panels				
Property		**Value**		
Distance between ribs		445 mm (±2.5%)		
Height of the cells		150–200 mm (±5%)		
Dimensions of the open cell		340 × 290 mm (±3%)		
# of cells/m^2		22		
Expanded section size		2.8 × 10.7–17.3 m (±3%) (máx.)		
Expanded section area		30–48 m^2 (±3%)		
Categories of the geocell				
Property	**Norm**	**Cat. A**	**Cat. C**	**Cat. D**
Resistance to welding (kN/m)	ISO 13426-1	9	15	18
Ultimate resistance of the material (MPa)	ASTM D638, ISO 527	22	24	28
Ultimate resistance (wide strip with perforations) (kN/m)	ISO 103192	9	15	22
Dimensional stability	Norm	Value		
Coefficient of thermal expansion (ppm/°C) measuring range of −30°C to +30°C	ASTM E-831	≤95		

Dimensions of the cells and panels		
Property		**Value**
Time of induction to oxidation (OIT at 200°C) (mpn.) (virgin material before any modification)	ASTM D-3895	≥125
Resistance to ultraviolet degradation (HPOIT at 200°C) (min.)	ASTM D-5885	≥1250
Durability of the cell to long-term cyclical loads (pass)	Accelerated radial pressure test (TRI)	Cells, joints, and perforations remained intact without evidence of plastic deformation at the end of the cyclic loading
Efficiency of the internal friction angle	ASTM D-5321	≥0.84
Flexural module for each temperature (MPa)	ISO 672 ASTM E2254 (DAM)	
−40°C		>1150
−10°C		>1050
+10°C		>950
+30°C		>750
+45°C		>650
+60°C		>550
Reduction factor due to permanent deformation(creep)	ASTM D-6992 (SIM)	
5 years		<1.2
10 years		<1.4
25 years		<1.9
50 years		<2.9

Table 3.
Geocell of types 3 and 4 properties, Provider 3.

2.1 Sampling

All samples used came from polyolefin geocells available in the Colombian market. The sampling was conducted randomly from a bank of specimens supplied by the manufacturer. For the high-density polyethylene (HDPE) geocells, its polymer contents are not mentioned in this document, since it is known as high-density polyethylene in all the state of the art. While for the Neoloy® Geocell, no typology is obtained since its raw material is patented and there is no information about its polymer composition.

For the first type of HDPE polyolefin geocells from Provider 1, the properties are shown in **Table 1**.

For the second type of HDPE polyolefin geocells from Provider 2, the properties are shown in **Table 2**.

For the third type of polyolefin geocell from Neoloy® of Provider 3, the properties shown in **Table 3** are available, for categories A, C, and D.

3. Procedure of the test

The laboratory procedure is divided into three parts.

Part I: To start the test, it is necessary to take the measurements of the samples; for this reason the length, width, and thickness of the geocell must be taken.

Part II: The specimen is adjusted to the metal jaws, generating a total interaction between the geocell and the jaws (**Figure 1**), while **Figure 2** shows how the jaws should be placed on both the upper and lower halves to generate the desired load transfer.

Figure 1.
Adjustment of the sample to the clamp.

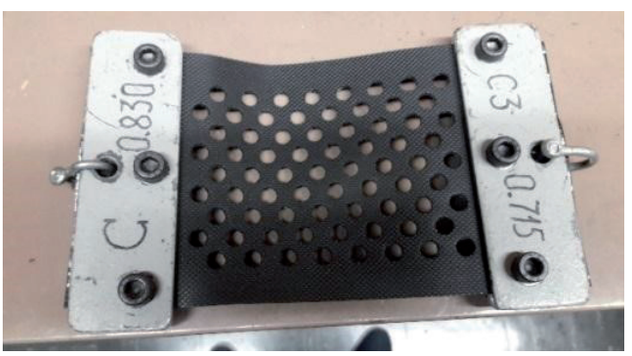

Figure 2.
Placement of the sample to the upper and lower jaws.

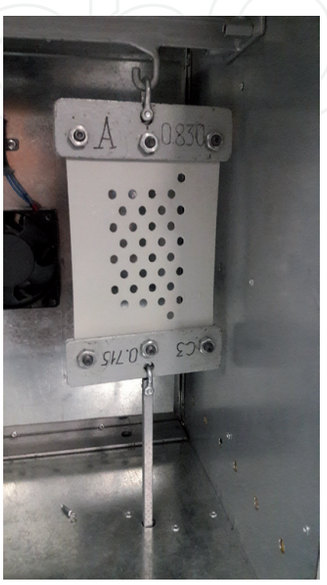

Figure 3.
Installation of the sample in the oven.

Figure 4.
Deformimeters in the base of the oven (left) and placement of weights in the stems (right).

Part III: In this step, the samples are hoisted in the oven support, complementing the union of the jaw of the lower part of the sample to the stem (**Figure 3**). After this it is necessary to place the deformimeters in the base that supports the oven (**Figure 4**, left).

Part IV: The hydraulic jack is placed in the lower part of the rods, generating a support so as not to exert preliminary efforts on the geocells, and then all the necessary weights are placed to reach the force required in the test (**Figure 4**, right). The oven is subsequently closed.

Part V: The oven is turned on at room temperature (21 ± 1°C), then the hydraulic jack is lowered by hanging the stems with the weights, and the first reading of the deformimeter is recorded, after which the steps with the pre-established times begun.

4. Results

To obtain the time-temperature superposition data that is necessary in the production of the SIM assay graphs, it was necessary to create an accurate graph, where equivalences (see **Table 4**) are determined between temperature and time superimposed by every minute that elapsed in temperature; see [10].

An exponential behavior is observed in these correlations, where time depends on temperature (**Figure 5**). For this reason, an exponential regression shown on the same graph is generated, in order to determine the total time that the geocell was exposed throughout the trial.

The following equation is the result:

$$T = 0.0005 * e^{0,3289 * t^{\circ}} \quad (2)$$

Temperature (°C)	Equivalent time (min.)
23	1
30	10
37	100
44	1000
51	10,000
58	100,000
65	1,000,000

Table 4.
Equivalent times.

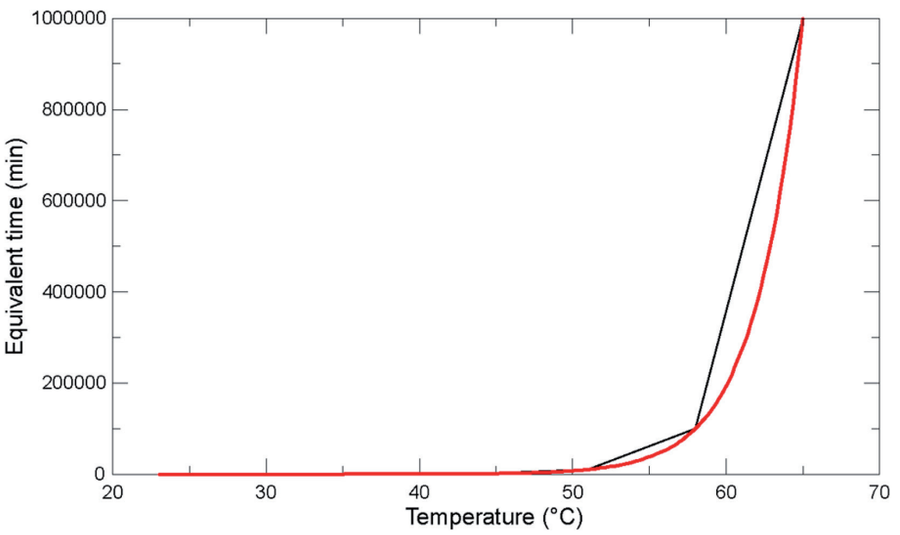

Figure 5.
Time-temperature superposition.

in which.

T: equivalent time in minutes per minute elapsed in temperature $t°$.

$t°$: temperature (°C).

The data for the time equivalent to the temperature were obtained based on the above equation, during the course of the different isothermal steps of the test. These equivalent times are shown in **Table 5**.

After the development of the different graphs made from the tests, it was possible to subtract and make a comparison between the materials that were used in each of the tests, in order to determine which behaved better in the long-term deformation. **Figure 6** shows the comparative graph of materials. A red line is again observed, which indicates 3% of the deformation, which generates a fault in the ground and the possible breakage of the pavement structure.

For the comparative graph of materials, the samples that had been exposed for a while were not considered, given that the other materials did not have this previous exposure and therefore leading to a possible erroneous comparison.

It is important to consider the effect that occurs in the geocells of Neoloy® from exposure to the environment (**Figure** 7), since these demonstrate the best behavior against long-term deformation [11–15].

Based on the previous results, it is important to make a new comparison in the Neoloy® Geocells, for its ultimate resistance to the wide strip test ISO 103192.

Step	Time (min.)	Accumulation of time (years)
Ambient	0	0
	30	2.96E−05
	60	5.91E−05
	90	8.87E−05
Increase to 44°C		
44°C	30	8.94E−03
	167	0.33
Increase to 51°C		
51°C	30	0.46
	167	3.63
Increase to 58°C		
58°C	15	4.94
	167	36.72
Increase to 65°C		
65 °C	60	78.78
	122	310.89

Table 5.
Equivalent times for the SIM test.

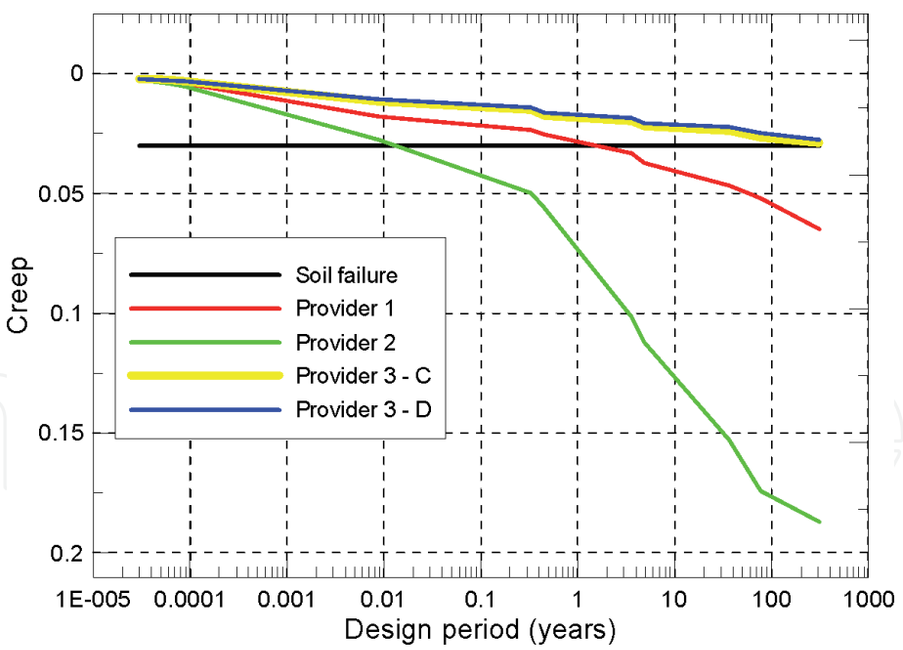

Figure 6.
Comparison of samples tested.

Figure 8 shows the incidence of this property in the behavior to the long-term deformation and the affectation on the MIF.

Continuing with the analysis of the behavior of the polyolefin geocells in long-term deformation, a different behavior was observed among the materials of the HDPE samples, where the thickness determined in part the behavior that was observed throughout the tests. Because of this, the evolution of the specimens in

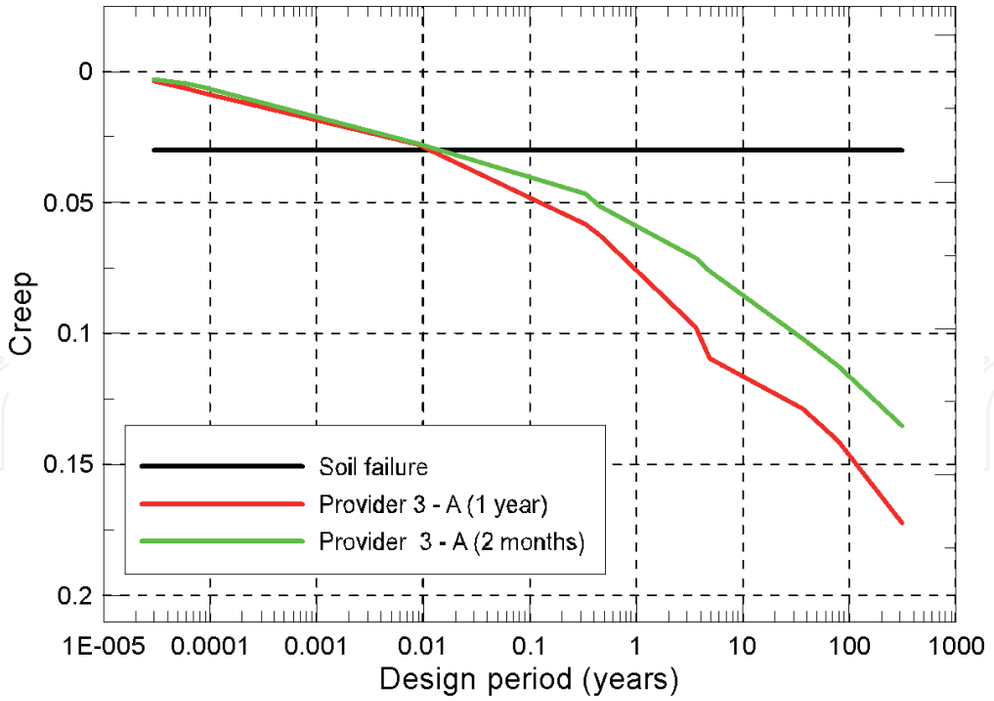

Figure 7.
Behavior according to environmental exposure time (Neoloy®).

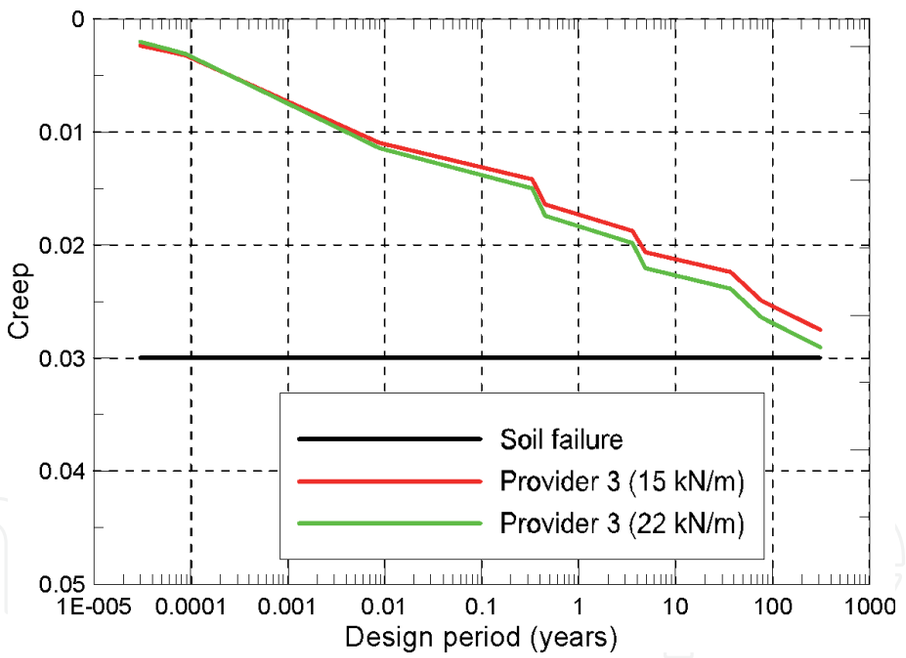

Figure 8.
Behavior of Neoloy® geocells according to resistance of wide strip ISO 103192.

terms of thickness is shown in **Figure 9**, revealing that the material with greater thickness presents a better response to this type of long-term stress.

As it is possible to extract from the different graphs in categories C and D composed of Neoloy® from Provider 3, an acceptable behavior was observed against the long-term deformation, this being the material that behaved better during the trials without reaching the 3% deformation failure in any of the two categories mentioned. Therefore, the geocells would have an MIF factor of high incidence in the module of the material to be confined, as shown in the Mohr circle (see **Figure 10**).

According to Han [16], the confinement creates an apparent cohesion considering the modification in the normal stresses caused to the granular material. This is

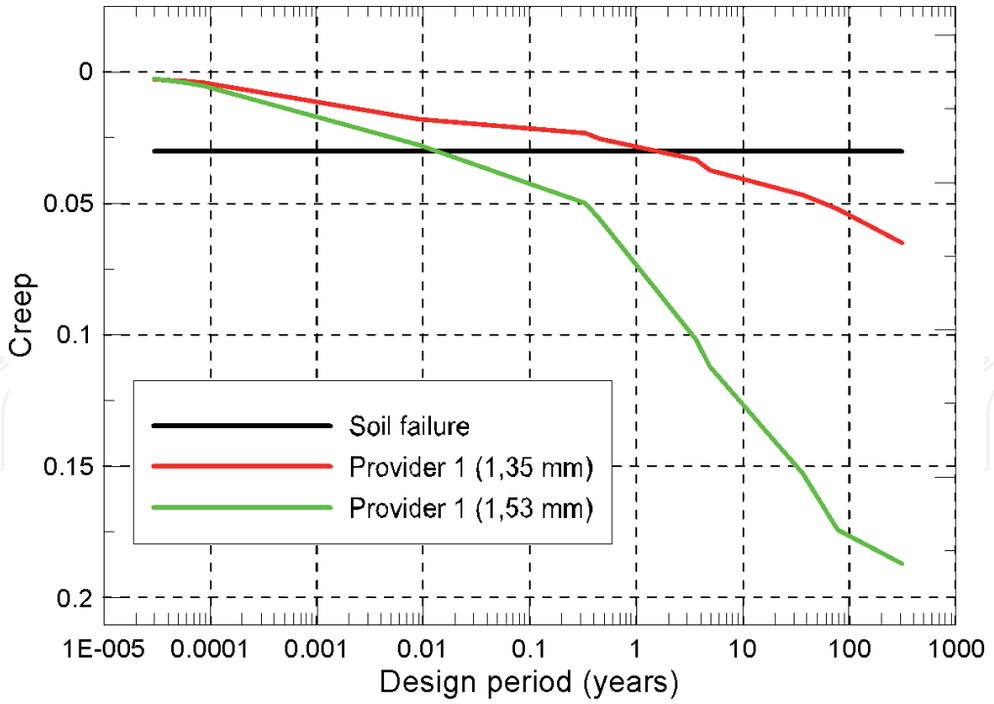

Figure 9.
Behavior HDPE geocells according to thickness.

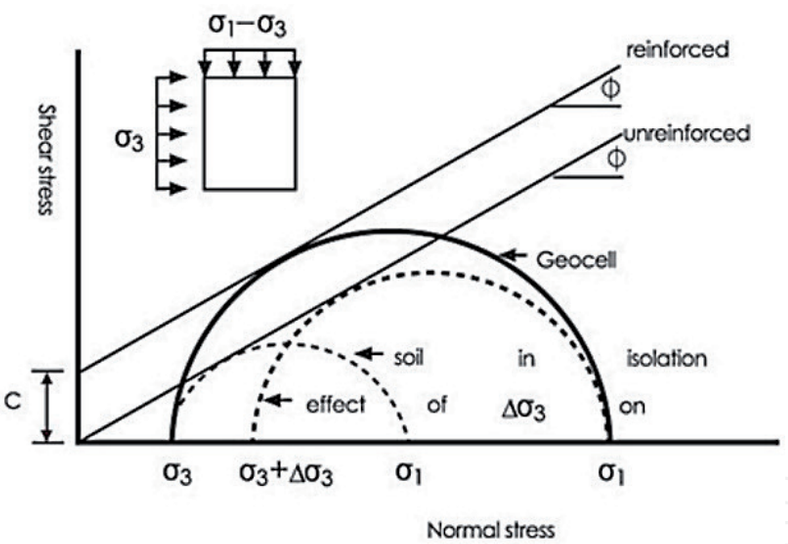

Figure 10.
Mohr circle of granular material with and without reinforcement [7].

only available if the material of the geocell resists the deformations produced by the stresses over the life of the project. Only the Neoloy® Geocells of categories C and D of Provider 3 manage to comply with the limitation of the MIFs.

When comparing the categories of the Neoloy® material, the great importance of both the thickness of the material and the resistance to the wide strip is observed. The results show better behavior in the geocell that has a greater resistance and greater thickness, displaying a high creep behavior and consequently increasing the MIF, which is significant when designing structures with this geocell methodology.

However, at the end of the tests, a rational time was determined to discharge the geocells. At this time an important behavior was observed in which the samples began to regenerate, decreasing the deformations that were at the end. The effect was established for the geocells that did not fail, showing an "elastic" behavior but

also maintaining a degree of plastic deformation. Therefore, a linear viscoelastic behavior can be determined, in which there is an initial elastic deformation caused by the stresses generated upon it, followed by a time-dependent delayed deformation, known as material creep. There may be some permanent flow in the material, especially when high loads are applied.

When the unload is permitted to the material, within linear viscoelastic behavior, an inverse process begins, with a certain recovery at the moment, continued by a recovery along the time recovering fluence dependent on the time. The material may or may not reach the original dimensions. If permanent flow occurs in the charging process, there will be a residual deformation even when the load application is no longer allowed [17–19].

5. Conclusions

Polyolefin geocells can be considered an excellent reinforcement in the structures of the roads as long as they meet certain specifications, such as resistance to long-term deformation. For the geocells tested, the best performance was obtained by the Neoloy® composite material.

Taking into account the results of the laboratories, the increase factor of MIF modules is directly connected to creep resistance. When confinement is eventually lost due to large deformations in the geocells, the increase will be zero, and the behavior of the granular material belonging to the pavement structure will be the same as if it were not considered reinforced, decreasing its modulus, requiring a greater thickness to comply with the conditions of the structure.

All polymeric material that is exposed to weather, for greater resistance that it possesses, suffers the loss of properties. This could be evidenced when comparing tests with the same material and category, but with different time of exposure to the effects caused by nature (UV rays, air, water, etc.). A lesser deformation was displayed in the sample that had been under condition for a year.

The deformation behavior of HDPE exposed to high temperatures is low compared to Neoloy® material. For this reason, it could be determined that the HDPE geocells, although they have a regular behavior, cannot be located in the base layer of the pavement structures, since these could have temperatures as tested in the "SIM test" or higher, generating a double deformation. One of them would be due to time and the other due to temperature, leading to failure in a very short period of time.

To determine the MIF, it is necessary to know the resistance of the material of the geocell to the long-term deformation, since it is a vital part of achieving high performance, during the entire life of the structure of pavement reinforced with geocells.

The geocells, composed by Neoloy® with a resistance to the wide strip of 15 kN/m, are the most suitable to achieve a subgrade improvement. These geocells have the ability to be used in the granular layers adjacent to the asphalt folder, decreasing thicknesses. The use of these minimum aspects is recommended to guarantee the functionality, serviceability, and long-term operability of structures where geocells are involved.

Author details

Juan Carlos Ruge[1*], Julian Gonzalo Gomez[1,2] and Carlos Andres Moreno[2]

1 Catholic University of Colombia, Bogotá, Colombia

2 Fluent Business Group, Mexichem Colombia S.A.S, Bogota, Colombia

*Address all correspondence to: jcruge@ucatolica.edu.co

References

[1] Geoceldas SA. Historia [Internet]. 2015. Available from: http://www.geoceldas.com/historia [Accessed: 12 April 2017]

[2] PRS Geo-Technologies. PRS stabilizing an unstable world. SIM Test Procedures ASTM D-6992. s.l.: PRS Technical Description; 2016

[3] PRS Geo-Technologies. The effect of creep on geocell design life. s.l.: PRS; 2015

[4] ASTM D6992-16. Standard Test Method for Accelerated Tensile Creep and Creep-Rupture of Geosynthetic Materials Based on Time-Temperature Superposition Using the Stepped Isothermal Method. West Conshohocken, PA: ASTM International; 2016

[5] ASTM International. Standard Terminology for Geosynthetics. Conshohocken: ASTM; 2004

[6] Pavco Mexichem. Manual de diseño con geosintéticos. Bogotá, D.C.: Pavco Mexichem Soluciones Integrales; 2012

[7] Herminda EB. Análisis de la superposición Tiempo-Temperatura: Determinación e interconversión de espectros de relajación y retardo. Buenos Aires: Universidad de Buenos Aires—Facultad de Ciencias Exactas y Naturales; 1991

[8] Billmeyer F Jr. Ciencia de los Polímeros. Barcelona, Reverté; 2004. ISBN: 84-291-7048-0

[9] PRS Geo-Technologies. PRS-Neoweb geocells (tough cells) test specification. PRS Geo-Technologies; 2017

[10] Tsorani G. Geoceldas en la ingeniería. Bogotá: PRS Geo-Technologies; 2017

[11] Kolathayar S, Suja P, Nair V. Performance evaluation of seashell and sand as infill materials in HDPE and coir geocells. Innovative Infrastructure Solutions. 2019;**4**:17. DOI: 10.1007/s41062-019-0203-6

[12] George AM, Banerjee A, Puppala AJ, Saladhi M. Performance evaluation of geocell-reinforced reclaimed asphalt pavement (RAP) bases in flexible pavements. International Journal of Pavement Engineering. 2019:1-11. DOI: 10.1080/10298436.2019.1587437

[13] Keshmiri N, Ghareh S, Kazemian S, Hosseinian A. 3D numerical analysis of loading geometry on soil behavior reinforced with geocell element. Journal of Testing and Evaluation. 2019;**47**(3). DOI: 10.1520/JTE20180194. ISSN: 0090-3973. Special Issue Paper

[14] Venkateswarlu H, Ujjawal KN, Hegde A. Laboratory and numerical investigation of machine foundations reinforced with geogrids and geocells. Geotextiles and Geomembranes. 2018;**46**(6):882-896

[15] Pokharela SK, Leshchinsky HD, Parsons RL. Experimental evaluation of geocell-reinforced bases under repeated loading. International Journal of Pavement Research and Technology. 2018;**11**(2):114-127

[16] Han J. Geocell reinforced research. Kansas City: University of Kansas; 2008-2012

[17] Álvarez FB. Comportamiento reológico de los polímeros. Viscoelasticidad. Universidad de Oviedo—Escuela de Minas de Oviedo; 2013

[18] Jeon H-Y. Review of Long-Term Durable Creep Performance. Creep. IntechOpen; 2017. doi: 10.5772/intechopen.72330

[19] Yeo SS, Hsuan YG. Predicting the creep behavior of high-density polyethylene geogrid using stepped isothermal method. In: Martin JW, Ryntz RA, Chin J, Dickie RA, editors. Service Life Prediction of Polymeric Materials. Boston, MA: Springer; 2009